Proceedings of the Canadian Society for Mechanical Engineering International Congress
32nd Annual Conference of the Computational Fluid Dynamics Society of Canada
Canadian Society of Rheology Symposium
CSME/CFDSC/CSR 2025
May 25–28, 2025, Montréal, Québec, Canada

NUMBER

The Impact of Membrane Thickness on IPMC Actuation Dynamics - A Simulation Study

Yu-Tung Chen[1], Kamran Behdinan[2]

[1]Department of Mechanical and Industrial Engineering, Faculty of Applied Sciences and Engineering, University of Toronto, Toronto, Canada
[2]Advanced Research Laboratory for Multifunctional Lightweight Structures (ARL-MLS), Department of Mechanical and Industrial Engineering, University of Toronto, Toronto, Canada

***Abstract*—**Ionic polymer-metal composites (IPMCs) are widely studied for their potential in soft actuation applications due to their ability to exhibit large bending displacements under low applied voltages. While prior research has extensively explored the impact of geometry on actuation force and displacement, the influence of membrane thickness on actuation dynamics, particularly reaction time and back relaxation behavior, remains underexplored. This study investigates the effect of membrane thickness on IPMC actuation performance using a multiphysics simulation approach. A finite element model based on an established electromechanical framework is implemented to capture the transient response of IPMC actuators with varying thicknesses. Simulation results show that increasing membrane thickness reduces both maximum and steady-state displacement due to increased bending stiffness. Furthermore, thicker membranes exhibit longer reaction times and more pronounced back relaxation, suggesting that relaxation dynamics are primarily diffusion-limited.

***Keywords-component*—IPMC; Soft Actuators, Multiphysic Simulation; Finite Element Analysis (FEA); Membrane Thickness, Back Relaxation**

I. INTRODUCTION

Ionic polymer-metal composites (IPMC) are a type of smart material that deforms under electrical stimulation. Their ability to exhibit large displacement under lower voltages makes them a promising candidate as artificial muscles, soft robotic actuators, as well as biomimetic sensors due to its ability to generate electrical signals under mechanical load [1], [2].

IPMC actuator mainly consists of an ion exchange membrane, typically Nafion or Flemion [3], [4], and two metal electrodes plated on both sides of the membrane. The bending behaviour of IPMC actuators stems from their ion-exchange process, where cations migrate across the ionomer in response to an electric field [2], [5], [6]. As the cations migrate to one side of the electrode, the free water molecules and water molecules attached to the cations also move towards the electrode, causing the material to expand or contract asymmetrically, resulting in bending deformation.

Despite their promising characteristics, the application of IPMC actuators is still limited by several factors, including back relaxation when subjected to direct current (DC) voltage, low actuation force, and solvent evaporation [2], [7]. These challenges highlight the need for further research and development to optimize their performance for practical applications. Researchers have explored various strategies to improve actuation performance, targeting both back relaxation and mechanical limitations.

One major limitation of IPMC actuators is back relaxation, a phenomenon where the actuator slowly returns to its original position even under an applied voltage. To mitigate this issue, researchers have investigated solvent modifications, such as replacing water with ionic liquids, which exhibit reduced evaporation and enhanced long-term stability [8], [9]. Additionally, the water content in the membrane has been found to significantly influence back relaxation, where higher water content often leads to stronger relaxation effects [10], [11].

Another major challenge with IPMCs as actuators is their low actuation force. To address this, mechanical reinforcement techniques have been investigated. Researchers have incorporated nanoparticles, such as carbon materials [12] and nanopowders [13], into the ion-exchange membrane, improving both its mechanical and electrical properties.

Apart from material modifications, the geometry and shape of the actuator also play a crucial role in actuation performance. Significant efforts have been made to manipulate membrane thickness to enhance actuation force [14], [15]. However, increasing thickness has been found to reduce the

level of displacement, presenting a trade-off between force and deformation. Conversely, modifying the membrane length has been shown to increase displacement, offering another approach to optimizing performance. While significant effort has been devoted to investigating the effect of membrane geometry on actuation properties, there has been limited research on how membrane thickness influences the dynamic interaction between electrical and mechanical responses and its impact on the back relaxation phenomenon. This research aims to explore the effect of IPMC thickness on actuation performance, focusing particularly on reaction time and back relaxation behavior, using multiphysics simulation.

II. Method

The effect of membrane thickness on the actuation performance of Nafion-IPMC is studied through numerical analysis. The simulation is conducted using the 2D finite element method (FEM). The geometry of a typical IPMC actuator is based on a commercial Nafion membrane with a thickness of 0.18 mm and a length of 30 mm. To investigate the influence of thickness, simulations are performed for multiple thickness values. Using 0.18 mm as a single layer (1L), we simulate actuators with thicknesses corresponding to 1, 1.25, 1.5, 2, 4, and 6 layers.

A. Multiphysics Modeling Equations

The most accepted explanation for the actuation of water-based IPMC is the swelling theory. When voltage is applied, the counterions in the polymer membrane migrate toward the cathode. The migration of the counterions causes the water to redistribute, concentrating at the cathode. The imbalance in the distribution of charge and mass then causes the deformation of the membrane. To model the deformation of the water-based IPMC and capture the back relaxation behaviour observed in water-based Nafion-IPMC, the multi-physical model proposed by Zhu et al. [11] is adopted. The physical model framework can be divided into two processes: the transport of ions and water molecules, and deformation resulting from mass redistribution.

1) Ion and Water Molecules Transport: Poisson's equation (Eq. 1) and the Nernst-Planck equation (Eq. 2 and 3) are used to model the distribution of electrical potential and charge across the membrane [11].

$$\nabla^2\phi = -\frac{\rho}{\varepsilon} = -\frac{F(c_I - c^-)}{\varepsilon} \tag{1}$$

$$J_I = -d_{II}(\nabla c_I + \frac{Z_I F c_I}{RT}\nabla\phi) - N_{dI} d_{WW}\nabla c_W - c_I K\nabla p \tag{2}$$

$$J_W = -d_{WW}\nabla c_W - N_{dW} d_{II}(\nabla c_I + \frac{Z_I F c_I}{RT}\nabla\phi) - c_W K\nabla p \tag{3}$$

Where ϕ is the potential, ρ is the charge density, ε is the effective permittivity, J_i is the flux density of cations and water molecules in the polymer. c_i is the concentration of the cation and water molecules. p is the total water potential, F is the Faraday constant, R is the gas constant, T is the temperature, and K is the hydraulic permeability coefficient [11].

Since a single cation can no longer carry the same number of water molecules in regions of higher cation concentration compared to lower concentration areas, the dynamic drag coefficient (N_{dW} and N_{dI}) is adopted to account for this variation. According to the Onsager reciprocal relations, the dynamic drag coefficient is described as follows [11], where n_{dI} and n_{dW} are the static drag coefficients for cations and water, and c_{W0} is the initial water concentration:

$$N_{dI} = n_{dI}\cdot(\frac{c_I}{c_W} > \frac{c^-}{c_{W0}}) + \frac{c_I}{c_w}\frac{d_{II}}{d_{WW}} n_{dW}\cdot(\frac{c_I}{c_W} \le \frac{c^-}{c_{W0}}) \tag{4}$$

$$N_{dW} = n_{dW}\cdot(\frac{c_I}{c_w} \le \frac{c^-}{c_{W0}}) + \frac{c_w}{c_I}\frac{d_{WW}}{d_{II}} n_{dw}\cdot(\frac{c_I}{c_w} > \frac{c^-}{c_{W0}}) \tag{5}$$

Lastly, the mass continuity equation (Eq.6) is needed to complete the dynamic transport equation for water and cation.

$$\frac{\partial c_i}{\partial t} + \nabla J_i = 0, (i = I, W) \tag{6}$$

2) Stress Strain Analysis: In the flux equation, we see that the total water pressure in the cluster (p) also influences the mass distribution. The total pressure contains two parts: hydrostatic pressure and eigen stresses generated by the redistribution of liquid [11]. The total pressure within the cluster can be defined as:

$$p = p_h + \sigma^* \tag{7}$$

Hydrostatic Pressure:

Hydrostatic pressure is the fluid pressure exerted within the cluster spaces. The elastic stress of the polymer acting on the solid liquid surface (σ_e) fundamentally governs the hydrostatic pressure inside the cluster.

$$p_h = -\sigma_e \tag{8}$$

Due to the high cross-link density of the material, under small strain conditions, the mechanical behavior of Nafion can be approximated as a linear elastic material and modeled using the Neo-Hookean formulation, while ignoring its viscoelastic properties. Additionally, assuming isotropic expansion and contraction of the ionic clusters and treating the material as incompressible, the elastic stress can be defined. In the absence of any external mechanical stimulation, the following equation is derived in [11] assuming the deformation is only caused by internal stress:

$$-\sigma_e = \frac{E_{dry}}{3}((\frac{B}{B_0})^{-4} - (\frac{A}{A_0})^{-4}) \tag{9}$$

where E_{dry} is the elastic modulus of dry Nafion, and B and A are the outer and inner radius of the cluster. Since the radius of the cluster is related to the volume change of the water, Eq. 9 can be defined as a function of the volume fraction of water, w_v [11].

$$p_h = \frac{E_{dry}}{3}((\frac{1+w_v}{1+w_{v0}})^{-4/3} - (\frac{w_v}{w_{v0}})^{-4/3}) \tag{10}$$

Eigen Stresses:

Besides the hydrostatic pressure, eigen stresses including osmotic pressure and electrostatic stress also contribute to the distribution of water and cation. In [11], they proposed a simplified eigen stress equation by taking advantage of the opposite tendency between the osmotic stress and electrostatic stress within the membrane.

$$\sigma^* = -\varphi \frac{RT}{\overline{V}_W} ln(1 + \frac{c_I}{c_w}) \tag{11}$$

Where $\overline{V}_W$ is the partial molar volume of water and φ is the extended osmotic coefficient that ranges from negative to positive. In the case of a negative coefficient, it indicates that the influence of electrostatic stress is more significant and vice versa.

Lastly, changes in water content directly influence the volume strain of the material, leading to deformation. Since volume strain depends on water content, it can be expressed in terms of the volume fraction of water. The relationship between the volume strain (ε_V) and the volume change due to redistribution can be shown in the following equation [11]:

$$\varepsilon_V = \frac{1}{1 + w_{v0}} (w_v - w_{v0}) \tag{12}$$

According to the small strain assumption, the liner eigen strain (ε_{ii}) can therefore be obtained:

$$\varepsilon_{ii} = \frac{1}{3} \varepsilon_V \tag{13}$$

B. COMSOL Mulitphysics Setup

To investigate how membrane thickness affects the distribution of voltage and mass transfer, we employ the finite element method (FEM) using COMSOL Multiphysics. A numerical analysis is conducted to examine the mass transport distribution along the thickness direction of the IPMC material under an applied electric field. The partial differential equation (PDE) interfaces are used to implement Poisson's equation (Eq. 1) and the flux equations for cation and water transport (Eqs. 2, 3, and 6). To model the deformation of the IPMC, the solid mechanics interface with a plane strain assumption is implemented. The internal strain (Eq. 13) is induced using the initial stress/strain node. For simplicity, the effect of the electrode is omitted and is assumed to have perfect conduction.

To accurately capture variations near the electrodes, where concentration and potential gradients are more pronounced, mapped meshing is applied at the top and lower boundaries for refinement. Fig. 1 provides a schematic representation of the meshing strategy. One key objective of this study is to examine how thickness influences the back-relaxation phenomenon. To achieve this, we adopt the parameters reported in [11], which were specifically used to fit an experimental case that exhibits back relaxation. These parameters allow for the evaluation of thickness effects on both actuation performance and back relaxation. The selected parameters are listed in Table I.

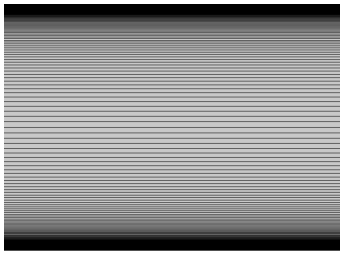

Figure. 1: Schematic representation of the mesh

TABLE. I: List of parameters used in simulation [11]

Variable	Value	Description
ε_r	8×10^{-10}	Effective permittivity
d_{II}	1.4×10^{-11} $[m^2/s]$	Diffusion coefficient of cation
d_{WW}	8×10^{-11} $[m^2/s]$	Diffusion coefficient of water
n_{dW}	4	Drag coefficient of water
n_{dI}	0.072	Drag coefficient of cation
w_{v0}	0.5368	Initial volume fraction of water
c^-	1393	Initial concentration of fixed anions
E_{dry}	1.6×10^9 [Pa]	Elastic modulus of dry Nafion-117
K	1.52×10^{-17} $[m^2/Pa \cdot s]$	Hydraulic permeability
φ	1	Osmotic coefficient
V	3 [V]	Applied voltage

C. Analysis Method

The time-dependent displacement of the IPMC actuator under a 3V step voltage input with a duration of 20 seconds is analyzed. The actuation performance is evaluated based on maximum displacement, steady-state displacement, reaction time, and back relaxation.

Displacement is measured at a point 15 mm from the fixed end of the beam, providing a straightforward method for quantifying deformation. For the steady-state displacement, The simulation was run until the displacement change within a 5-second interval was less than 0.5% to ensure steady-state conditions.

The reaction time represents the time it takes the actuator to reach maximum displacement. The time is determined by fitting the time displacement relationship with the exponential equation (Eq.14), where the characteristic time is used to represent how quickly the system rises. A similar approach is done to quantify back relaxation, where the displacement of the beam from maximum displacement to steady state is modeled with the exponential function, Eq.15, and the characteristic time is reported.

$$d(t) = disp_{initial} + (disp_{peak} - disp_{initial})(1 + e^{-\frac{t}{\tau}}) \tag{14}$$

$$d(t) = disp_{steady} + (disp_{peak} - disp_{steady}) e^{-\frac{t}{\tau}} \tag{15}$$

τ is the characteristic time that will be used to indicate the level of reaction and relaxation in each sample.

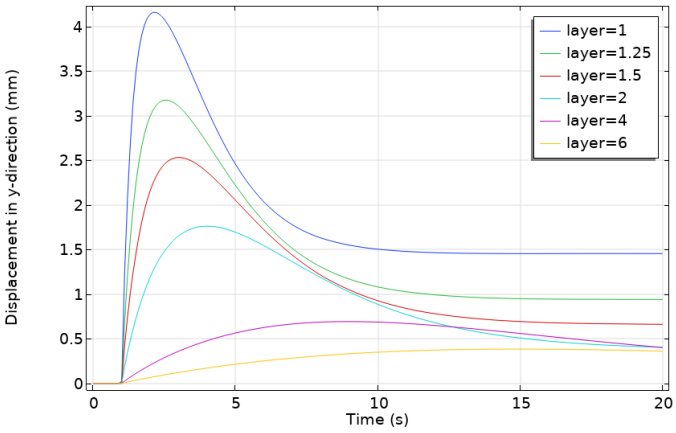

Figure. 2: Displacement over time

III. Result and Analysis

Fig.2 shows the generated displacement plot over time for each sample. The simulated result shows that as the thickness increases, the maximum and steady displacement both decrease. This outcome is expected since in theory the bending stiffness increases as the membrane thickness increases, hindering the actuator's ability to deform. The time-displacement plot reveals that thicker membranes also exhibit a slower reaction time, as the initial peak displacement occurs later compared to thinner samples. This delayed response suggests that the underlying transport processes, including ion migration and water diffusion, are affected by membrane thickness. Since the actuation response is driven by ion migration, examining the potential distribution provides insight into how membrane thickness influences charge transport and, consequently, reaction time and displacement.

Figure 3 shows the potential distribution across thicknesses 1L and 2L at different times. By comparing the potential profiles for samples with thicknesses of 1L and 2L, we observe that the induced potential in the thicker membrane takes longer to develop and stabilize. This delay in potential evolution confirms that increased transport resistance in thicker membranes hinders the rapid redistribution of cations and water molecules. Since the potential distribution is directly related to cation concentration, this slower charge movement contributes to the delayed mechanical response observed in the displacement plot. Additionally, comparing the potential distribution at steady-state (t=25s), the thinner membrane shows a thicker effective potential gradient layer relative to its thickness suggesting a stronger driving force for cation migration. This then also explains the larger displacement observed in the thinner membrane.

A. Trend

Fig.4 shows the maximum and steady displacement trend as thickness increases. The plot shows an inverse relationship between displacement and thickness. The obtained thickness displacement trend follows closely to the reported trend in literature [15], [16]. The Displacement vs. Thickness plot

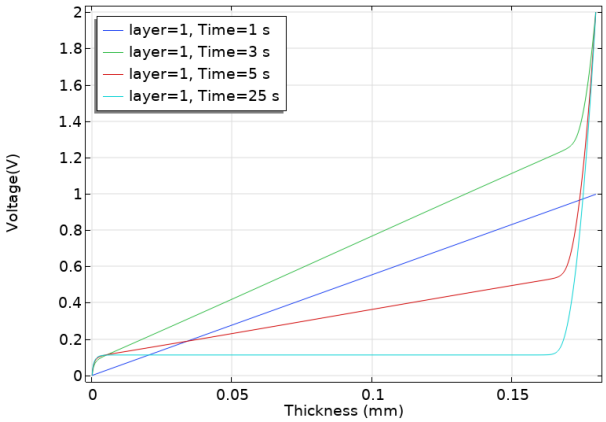

(a)

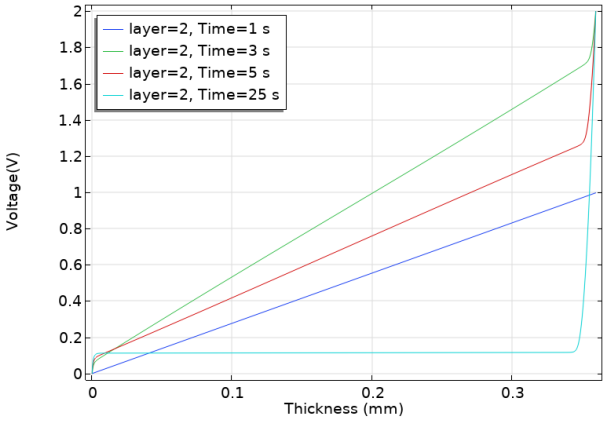

(b)

Figure. 3: Potential distribution across thickness for samples (a) 1L and (b) 2L

reveals a strong inverse relationship between membrane thickness and both maximum and steady-state displacement. As membrane thickness increases, displacement decreases following a power-law decay, as indicated by the fitted equation. The plot further reaffirms that thinner membranes experience larger actuation, while thicker membranes exhibit more restricted deformation due to the increased stiffness. Interestingly, the steeper exponent for steady-state displacement (-1.991) compared to maximum displacement (-1.329) implies that steady-state response is more strongly influenced by thickness.

From the perspective of back relaxation, this actually suggests that the thicker membrane experiences stronger back relaxation as the thinner membrane is able to retain more of its initial deformation as it relaxes. This could be explained by the lower effective potential across the thicker membrane and the thinner effective potential gradient layer mentioned in the previous section.

The plot of characteristic relaxation time (τ_{BR}) and reaction time (τ_R) as a function of thickness shown in Fig.5 reveals that both parameters increase with the membrane thickness but at different rates. τ_{BR} shows a much steeper increase, indicating that thicker membranes take significantly longer to fully relax

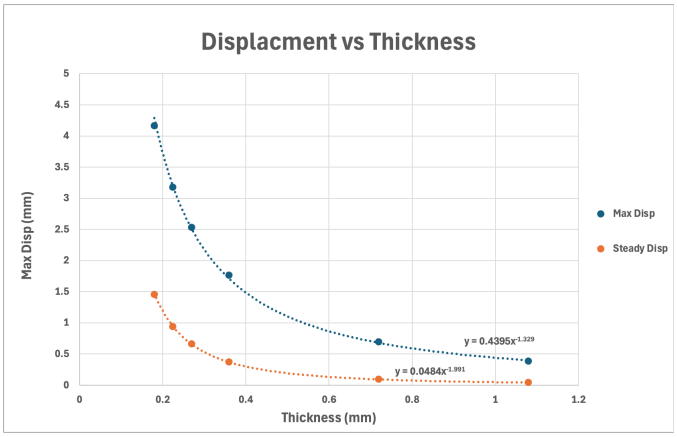

Figure. 4: Maximum and steady displacement of different thickness

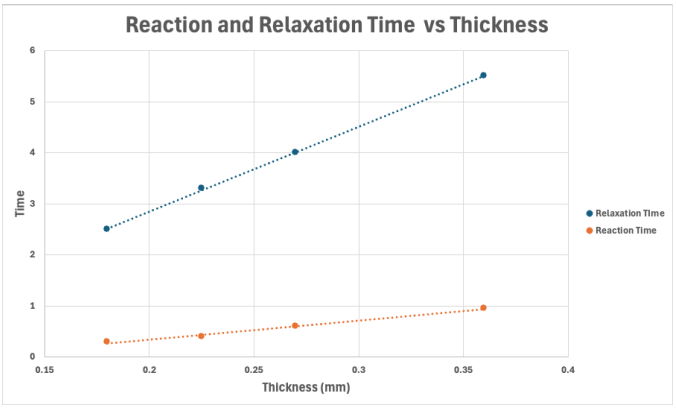

Figure. 5: Reaction and relaxation time with different thickness

after reaching peak displacement. In contrast, τ_R increases at a much slower rate, suggesting that while thicker membranes also take longer to reach maximum displacement, the effect of thickness on actuation time is much less pronounced compared to relaxation time.

The difference in the slopes of these two trends provides insight into the underlying transport mechanisms. The fact that τ_{BR} is more strongly influenced by thickness than τ_R suggests that back relaxation is more heavily influenced by diffusion limitations. As membrane thickness increases, the ion and water redistribution pathways become longer, significantly slowing down relaxation, which is likely governed by diffusion-driven charge and solvent migration. In contrast, the shallower slope of τ_R suggests that the initial actuation process is less diffusion-limited and may be more strongly driven by the applied electric field, allowing for a relatively faster response despite increasing thickness.

Oppose to the finding from the displacement trend, this suggests that back relaxation in thick membranes is not necessarily weaker but occurs over a much longer timescale. The strong dependence of τ_{BR} on thickness implies that relaxation does not simply depend on the initial displacement magnitude but is controlled by the diffusion time scale.

IV. Conclusion

This study provides a comprehensive numerical investigation of the effect of membrane thickness on the actuation performance of IPMCs, focusing particularly on reaction time and back relaxation. The results indicate that while increasing membrane thickness enhances actuation force, it significantly reduces displacement and prolongs both reaction and relaxation times. The observed trends suggest that back relaxation in thicker membranes is not necessarily weaker but occurs over a much longer timescale due to diffusion constraints. Additionally, the inverse relationship between displacement and thickness highlights the trade-off between actuation force and deformation. These findings offer valuable design considerations for optimizing IPMC-based actuators by tailoring membrane thickness to achieve desired performance characteristics.

V. Future Work

To further validate the simulation results, physical experiments should be conducted to systematically analyze the effect of membrane thickness on IPMC actuation performance. Current literature often reports thickness variations in larger intervals, making it difficult to capture the precise relationship between thickness and back relaxation behavior. A more granular experimental approach, using membranes with smaller thickness increments, would provide a clearer understanding of how thickness influences relaxation dynamics.

In this study, we assumed that membrane thickness does not significantly affect material properties, such as ionic conductivity, hydration level, or viscoelastic behavior, to isolate the mechanical and transport effects of thickness variation. However, in reality, material properties may also evolve with thickness due to differences in fabrication conditions, water retention, and crosslinking density. Future work could incorporate thickness-dependent variations in material properties to further improve the predictive accuracy of deformation trends.

While this study makes a significant contribution by isolating the effect of thickness under controlled conditions, incorporating additional material-dependent variations in future work would allow for a more comprehensive understanding of IPMC behavior. By integrating experimental validation with refined numerical models, future studies can improve the accuracy of IPMC simulations and provide deeper insights into optimizing actuator performance.

References

[1] M. Yu, H. Shen, and Z.-d. Dai, "Manufacture and performance of ionic polymer-metal composites," Journal of Bionic Engineering, vol. 4, no. 3, pp. 143–149, 2007.

[2] M. Hao, Y. Wang, Z. Zhu, Q. He, D. Zhu, and M. Luo, "A compact review of ipmc as soft actuator and sensor: Current trends, challenges, and potential solutions from our recent work," Frontiers in Robotics and AI, vol. 6, p. 129, 2019.

[3] A. Leronni, Modeling the Electrochemo-poromechanics of Ionic Polymer Metal Composites and Cell Clusters. Springer Nature, 2022.

[4] M. Shahinpoor, "Fundamentals of ionic polymer metal composites (ipmcs)," 2015.

[5] M. Shahinpoor, “Mechanoelectrical phenomena in ionic polymers,” Mathematics and Mechanics of Solids, vol. 8, no. 3, pp. 281–288, 2003.
[6] K. Schmidt-Rohr and Q. Chen, “Parallel cylindrical water nanochannels in nafion fuel cell membranes,” Nature materials, vol. 7, no. 1, pp. 75–83, 2008.
[7] K. Jung, J. Nam, and H. Choi, ”Investigations on actuation characteristics of IPMC artificial muscle actuator,” Sensors and Actuators A: Physical, vol.107, no.2, pp. 183-192, 2003
[8] W. Hong, C. Meis, J. R. Heflin, and R. Montazami, “Evidence of counterion migration in ionic polymer actuators via investigation of electromechanical performance,” Sens. Actuators B Chem., vol. 205, pp. 371–376, Dec. 2014
[9] M. D. Bennett, D. J. Leo, ”Ionic liquids as stable solvents for ionic polymer transducers,” Sensors and Actuators A: Physical, vol. 115, no. 1, pp, 79-90, 2004
[10] Y. Wang, H. Chen, Y. Wang, Z. Zhu, and D. Li, “Effect of dehydration on the mechanical and physicochemical properties of gold-and palladium-ionomeric polymer-metal composite (ipmc) actuators,” Electrochimica Acta, vol. 129, pp. 450–458, 2014.
[11] Z. Zhu, H. Chen and L. Chang, ”IPMC Actuation Mechanisms and Multi-physical Modeling,” Soft Actuators: Materials, Modeling, Applications, and Future Perspectives, pp. 455-502, 2019
[12] C. Li, E. T. Thostenson, and T. W. Chou, ”Sensors and actuators based on carbon nanotubes and their composites: a review,” Compos. Sci. Technol., vol.68 pp.1227–1249, 2008
[13] C. K. Chung, P. K. Fung, Y. A. Hong, M. S. Ju, C. C. K. Lin and T. C. Wu, ”A novel fabrication of ionic polymer–metal composites (IPMC) actuator with silver nano-powders,” Sensors Actuators B, vol. 117 pp. 367–375, 2006
[14] S. J. Lee, M. J. Han, S. J. Kim, J. Y. Jho, H. Y. Lee and Y. H. Kim, ”A new fabrication method for IPMC actuators and application to artificial fingers,” Smart Mater. Struct. vol. 15 pp. 1217–1224, 2006
[15] C. Oh, S. Kim, H. Kim, G. Park, J. Kim, J. Ryu, P. Li, S. Lee, K. No and S. Hong, ”Effects of membrane thickness on the performance of ionic polymer–metal composite actuators,” RSC advances, vol. 9, no. 26, pp. 14621-14626, 2019
[16] D. Vokoun, Q. He, L. Heller, M. Yu and Z. Dai, ”Modeling of IPMC cantilever’s displacements and blocking forces,” Journal of Bionic Engineering, vol.12, no. 1, pp. 142-151. 2015